Single-Point Scratching of 6061 Al Alloy Reinforced by Different Ceramic Particles

CHENG YAN and LIANGCHI ZHANG⋆
Centre for Advanced Materials Technology, Department of Mechanical and Mechatronic Engineering, University of Sydney, NSW 2006, Australia

Abstract. Aluminium alloys reinforced by ceramic particles have been widely used in aerospace and automotive industries for their high stiffness and wear resistance. However, the machining of such materials is difficult and would usually cause excessive tool wear. The effect of ceramic particles on the cutting mechanisms is also unclear.

The purpose of this study is to investigate the cutting mechanisms and the relationship between specific energy of scratching and depth of cut (size effect). The single-point scratch test was carried out on 6061 Al and its composites reinforced by Al_2O_3 and SiC ceramic particles using a pyramid indenter. The results indicated that the scratch process was composed of rubbing, ploughing, plastic cutting and reinforcement fracture. A simple model was proposed to interpret the apparent size effect. The effect of reinforcement on the specific energy was correlated to the ratio of volume fraction to particle radius. The paper found that for machining MMCs, a larger depth of cut should be used to maintain a lower machining energy, especially for those with a larger ratio of volume fraction to particle radius.

Key words: Metal matrix composites, Reinforcement effect, Scratching, Specific energy, Size effect, Groove topography, Depth of cut.

Nomenclature

A	area,
C	length or radial crack,
C_0, C_1, C_2, C_3	constants in Equations (3), (4), (5), and (9),
E	Young's modulus,
f	friction coefficient,
f_ν	volume fraction of particles,
F_t	tangential force,
H	Vicker's hardness,
h	depth of cut,
K_c	fracture toughness,
K	constant in Equation (7),
L	groove length,
L_e	total edge length of particles, defined in Equation (11),

---

⋆ Author to whom correspondence should be addressed.

P	indentation load,
p	average contact pressure,
R	particle radius,
α, α_1	constants, defined in Equations (6) and (8),
γ	surface energy of particles,
θ	semi-included angle of groove,
μ	specific energy,
ξ	ratio of particle volume fraction to average radius of particles,
σ_y	yield stress of a composite material,

subscript

c	plastic cutting,
f	fracture,
g	groove surface,
p	ploughing,
r	rubbing,
s	section of groove.

1. Introduction

It is well known that metal matrix composites (MMCs) have considerable potential of enhanced strength and abrasive wear resistance [1–5]. However, because of the extremely different behaviour of the two phases involved, the hard particles and the soft matrix, the machining of MMCs, such as turning, milling and grinding, is often knotty, causing significant tool wear and unstable quality of machined surfaces. Nevertheless, it has been found that the specific machining energy is an important parameter correlating to tool wear, temperature distribution and surface quality of workpieces in all the above machining processes [6, 7]. The relationship between the specific machining energy and depth of cut(size effect) has been widely used for investigating the machining of single phase materials. Backer et al. [8] found that there was a significant increase in specific energy as chip thickness decreased to about $20\,\mu$m when grinding SAE 1112 steel, because crystal defects would have less and less effect on the shear strength of the work materials. A similar size effect was reported [9, 10] in scratching or grinding ductile and brittle materials. However, the work of Nakayama et al. on copper cutting [11] showed that the shear strength did not increase even when the chip thickness became very small ($2\,\mu$m). Malkin et al. [12] proposed that the size effect was mainly related to the relative energy contributions of sliding, ploughing and chip formation. These studies demonstrate that the specific machining energy is a function of at least two groups of factors: the properties of a workmaterial and the parameters set for a specific machining process.

On the other hand, the machining of MMCs is similar, to a great extent, to an abrasive process of a wear system. Therefore, studies of abrasive process involving MMCs are also very useful. It has been recognised that the effect of

the hard reinforcement on abrasive wear resistance can be interpreted in terms of decreasing the dimensionless wear coefficient [1] and that a higher volume fraction of ceramic reinforcement and a larger particle size provide greater abrasive wear resistance [1, 4]. Wang and Hutching [5] illustrated that there existed an optimal volume fraction of reinforcement and fine particles should usually be used for generating a high abrasion resistance. Therefore, the understanding of the effect of the size and the volume fraction of reinforcement on abrasive wear mechanisms is far insufficient [13]. The question to be answered is what is the main role of the ceramic reinforcement in an abrasive process of a MMC material in terms of its size and volume fraction, though ceramic particles increase the compound hardness of the composite in general.

Accordingly, for MMCs, the quantity of specific energy could also be an important variable in exploring the mechanisms of abrasive wear and determining optimal machining conditions. Unfortunately, relevant researches are few and in-depth understandings are lacking.

This paper addresses the single-point scratch test of 6061 Al and its composites reinforced with Al_2O_3 and SiC particles. Emphasis is placed on the cutting mechanisms and the relationship between the specific energy of scratching and depth of cut.

2. Experimental Procedure

The materials investigated were 6061 Al and its composites reinforced by 10% and 20%(wt%) Al_2O_3/SiC particles of different sizes. For simplicity, those reinforced by 10% Al_2O_3, 20% Al_2O_3, 10% SiC and 20% SiC will hereafter be referred to as AO10, AO20, SC10 and SC20, respectively. The materials were solution heat treated at 530 °C for 2 hours followed by a water quench and aging at 175 °C for 8 hours. This process is known in engineering practice as T6 treatment. In order to investigate the effect of T6 treatment on the material hardness and cutting process, some materials were received in as-extruded condition without heat treatment. All specimen surfaces were polished before testing using a diamond paste with grits of an average diameter of 1 μm. To obtain reliable hardness values, the Vicker's hardness of each material was measured at different loads. The volume fraction, average particle diameter, and average free path of ceramic particles were measured by an image analysis system (Leica microscope with md30 software). The scratch tests were carried out using a reciprocating scratch machine with a constant scratching speed of 6 mm^{-1} s. The apex angle of the pyramid indenter used was 136°. The normal load applied varied from 2.5 to 20 N to obtain different depths of cut. The tangential forces were measured by a force transducer. The surfaces of the grooves formed were observed under scanning electron microscope (SEM). For calculating the volume of the material removed, the width and depth of the grooves were measured using a laser confocal microscope.

3. Results and Discussion

3.1. MICROSTRUCTURES AND VICKER'S HARDNESS

The initial microstructure of the work materials are shown in Figure 1. The profiles of the particles are irregular and their distribution in the matrix are random. The volume fraction, average diameter, average free path of particles and the ratio of volume fraction to particle radius (ξ) are listed in Table I. The Al_2O_3 particles have a larger average diameter and average free path but a smaller ξ compared to SiC particles. SC20 has the smallest average free path but the largest ξ value among all materials. The variation of Vicker's hardness of all the
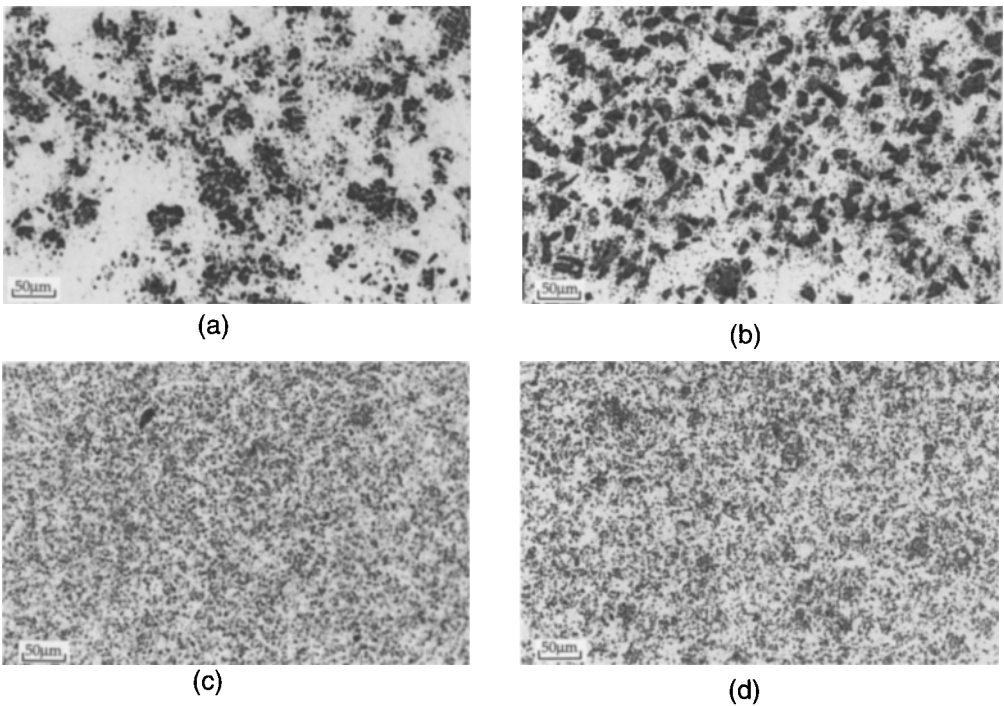
Fig. 1.   Initial microstructure of materials (a) AO10, (b) AO20, (c) SC10 and (d) SC20.

TABLE I. Metallographic parameters of the particle reinforcement

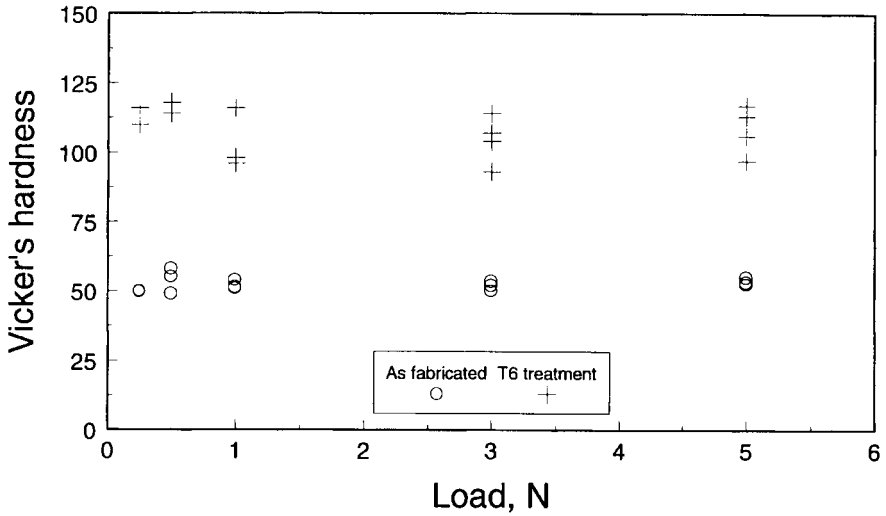|	AO10	AO20	SC10	SC20
Average diameter (μm)	14.40	18.39	3.70	3.51
Volume fraction (%)	15.83	27.42	14.99	24.90
Weight fraction (%)	10.00	20.00	10.00	20.00
Average free path (μm)	76.60	48.70	20.90	10.60
ξ	2.20	2.90	8.10	14.20

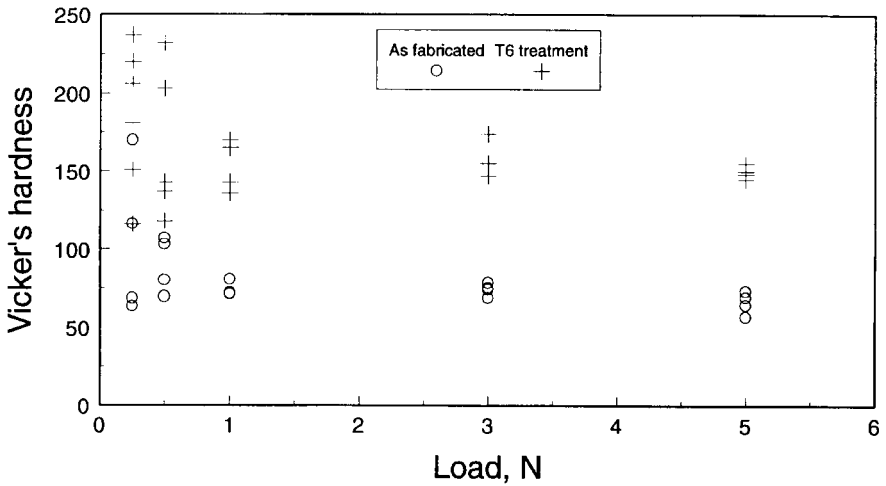Fig. 2a.   Variation of hardness with applied loads: 6061 Al.

Fig. 2b.   Variation of hardness with applied loads: AO10.

materials with indentation load, heat treatment and type of reinforcement is shown in Figure 2. It is obvious that both solution treatment (T6) and reinforcement increase the hardness of a composite. For 6061 Al, the hardness is independent of applied load (Figure 2a) because the material is homogeneous, isotropic and less work hardening such that the geometrical similarity applies under different indentation loads. For all the composites, however, a large scatter of hardness is
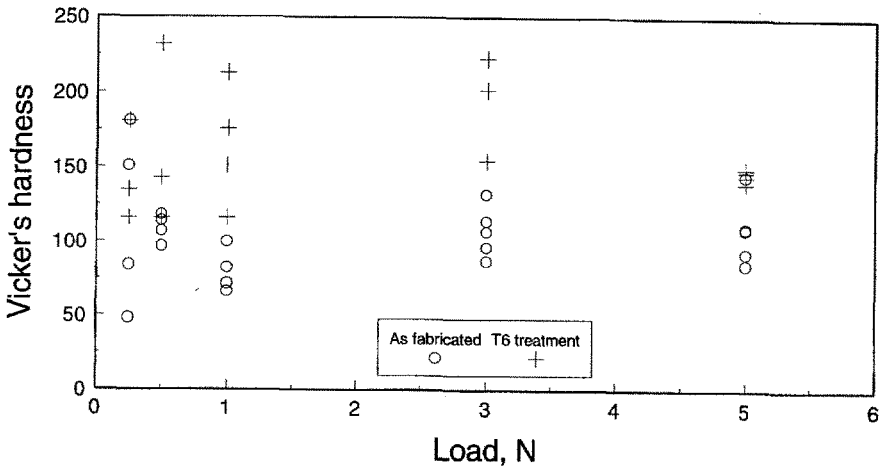
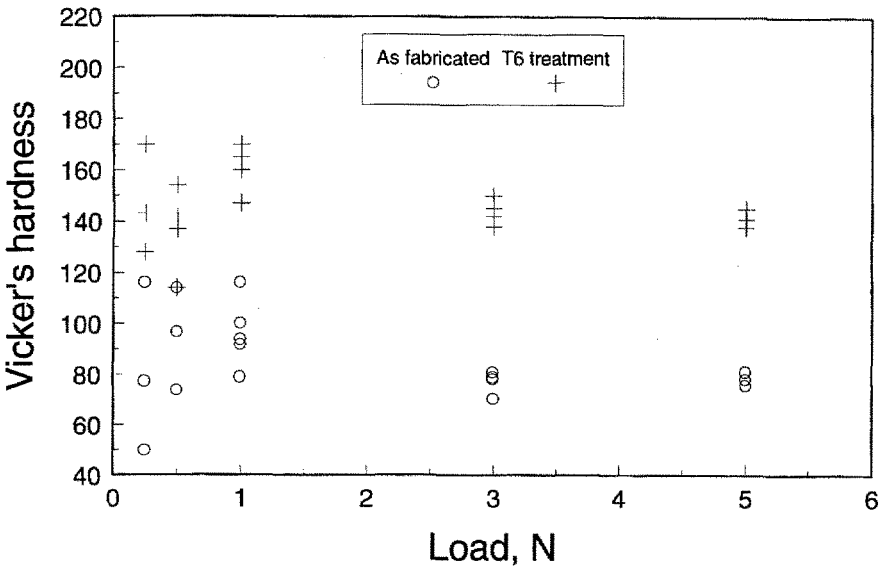Fig. 2c. Variation of hardness with applied loads: AO20.

Fig. 2d. Variation of hardness with applied loads: SC10.

observed when the indentation load is small, Figures 2b–e. It is not difficult to understand if the microstructure of the composites is taken into account. When the indentation load is small, the identation depth is small as compared to the average diameter of the particles. Thus the hardness reading would greatly be affected by the random distribution of the particles, or in other words, by the
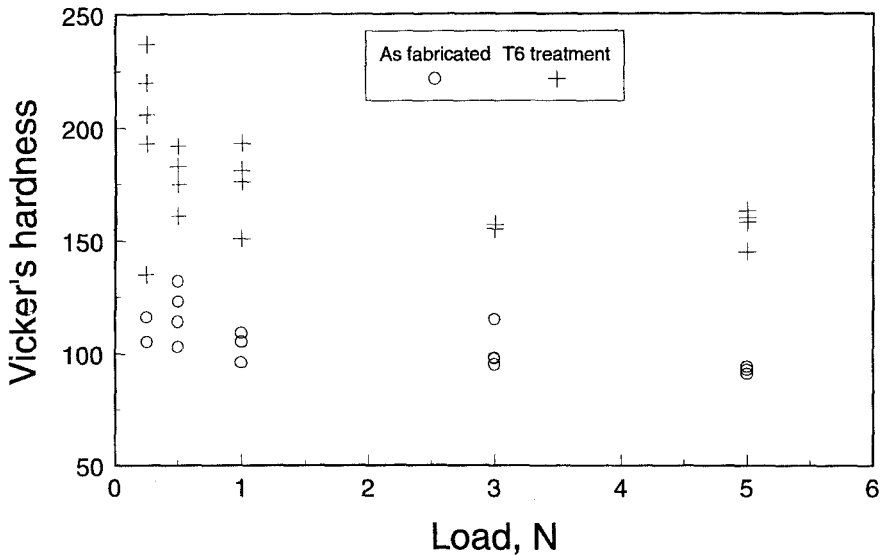
Fig. 2e.   Variation of hardness with applied loads: SC20.

identation position on the workpiece surface. When the load becomes large, the contact zone of indentation is large and covers many particles. In this case, the properties of matrix, particles and particle-matrix bonding, all together, provide a stable hardness response.

The compound hardness of a composite is an important parameter in modelling its wear and machinability. According to the above observations, the selection of indentation load for the hardness measurement must therefore be carefully related to its specific application. For instance, if the hardness of a composite to be measured is for estimating its machinability or wear rate in a system with an average depth of asperity penetration x, then the best indentation depth for such hardness measurement should also be x.

3.2. GROOVE TOPOGRAPHY AND CUTTING MECHANISMS

Figure 3 presents the groove topography of 6061 Al, with and without T6 treatment, at different normal loads. The groove and ridges were irregular when the load is small (2.5 N), Figure 3a, but become regular and smooth when it is large (e.g., 15 N), Figure 3b. Heat treatment alters the groove formation as well. The groove of 6061 Al with T6 treatment (Figure 3c) is clearly smoother than that without such treatment (Figure 3b) at the same load (15 N). Based on the studies of scratching metals [14, 15], the formation of grooves and ridges is the result of rubbing, ploughing and plastic cutting. However, each component plays a different role under a certain depth of cut. Rubbing is a significant factor when

(a)P=2.5N, without T6 treatment

(b)P=15N, without T6 treatment

(c) P=15N, after T6 treatment

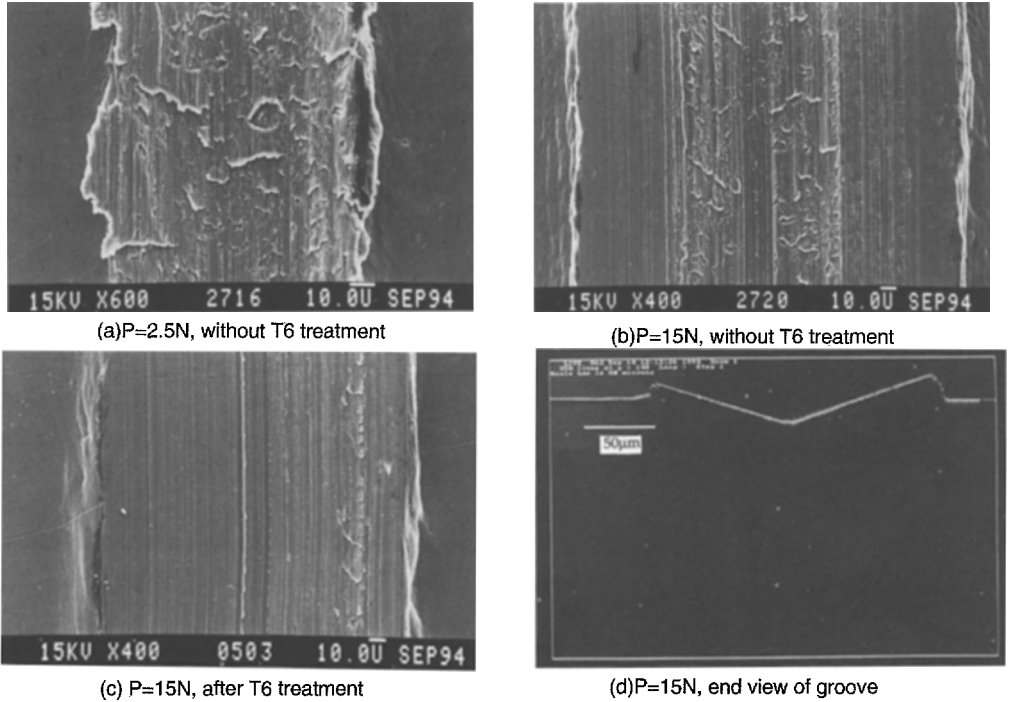(d)P=15N, end view of groove

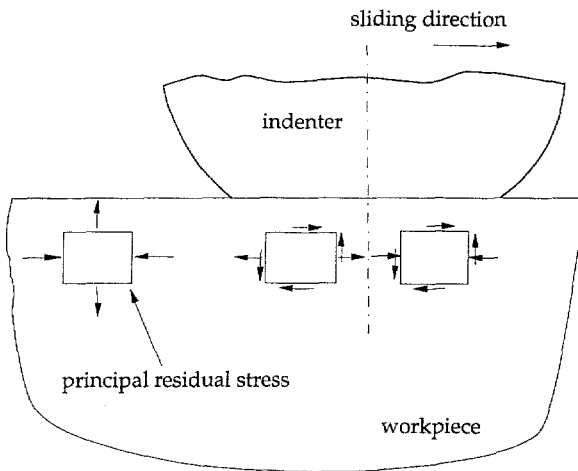Fig. 3.   Groove topography of 6061 Al.

Fig. 4.   Schematic stress distribution beneath a sliding contact.

the depth of cut is small but becomes less important when it is large. With the increase of depth of cut, ploughing and plastic cutting govern the process successively and make the groove surface smoother. An interesting fact was that some

(a)SC20, P=2.5N

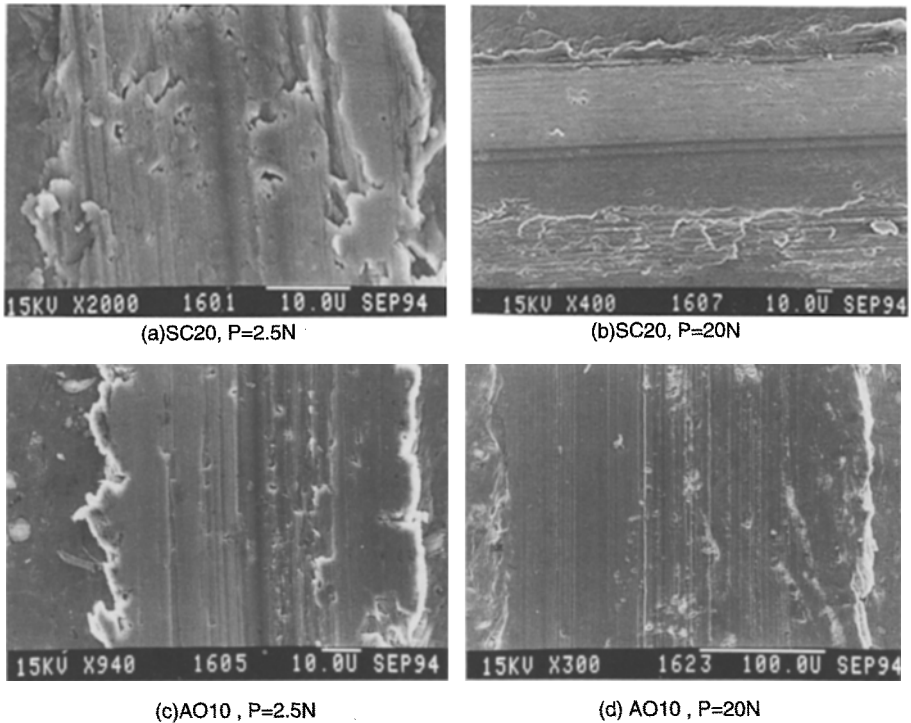(b)SC20, P=20N

(c)AO10 , P=2.5N

(d) AO10 , P=20N

Fig. 5.   Groove topography of composites AO10 and SC20.

scales formed at the bottom of the groove, Figure 3b, which is not desirable in any machining operation. This is due to the special stress and residual stress distributions during the sliding of the indenter over the workmaterial. When the indenter is sliding on the workmaterial surface, rubbing, ploughing and plastic cutting all produce a horizontal compressive stress on the workmaterial surface in front of the indenter but a corresponding tensile stress behind it [16]. The tensile stress would easily cause surface cracking. Moreover, an investigation of indentation [17] revealed that the tensile principal residual stress in the workmaterial is almost perpendicular to the surface and the compressive one parallel to it, Figure 4. Such a residual stress state can make the cracks propagate easily in the sliding direction. Hence, the appearance of the scales are understandable. However, the number and the size of the scales must be very dependent on the interface conditions of scratching. Larger and longer scales indicated a higher interface friction and a lower normal scratching load. This is well confirmed by Figure 3a–c. The scales did not tend to appear when the material properties were changed after T6 treatment that altered the friction behaviour of the material (Figure 3c).

The variation of the groove topography of the composite materials are similar, to a certain extent, to that of 6061 Al discussed above (Figure 5). The grooves are not very regular and not smooth at small normal loads (Figure 5a and c)
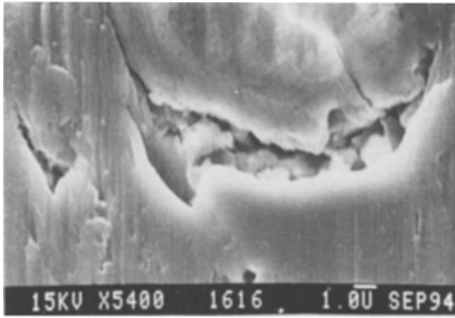
(a)AO10, P=2.5N
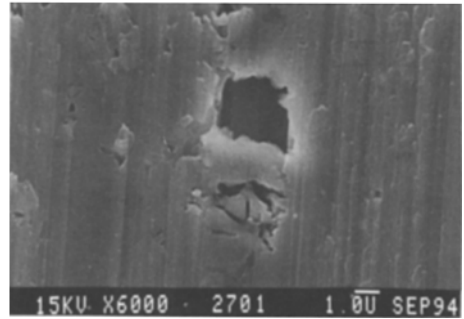
(b)SC20, P=6N

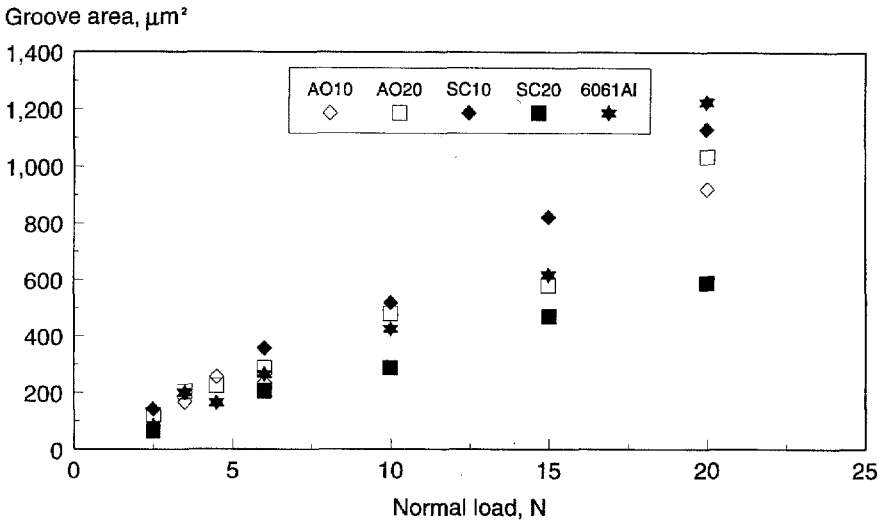Fig. 6.   Fractured particles on groove surfaces.

Fig. 7.   Variation of groove area with normal load.

and become regular and smooth when the load increases (Figure 5b and d). However, a distinctive character is the fractured Al_2O_3 and SiC particles on the groove surface (Figure 6). Clearly, the ceramic particles were either fractured or dug out by the passing indenter. Therefore, for composites with brittle reinforcements, besides rubbing, ploughing and plastic cutting, particle fracture is also an important component in groove formation. The relationship between the groove area and normal load is indicated in Figure 7. In general, SC20 has the smallest groove area an therefore has the greatest abrasive wear resistance. The size and volume fraction effects of the reinforcement on scratching process will be discussed later.

3.3. SPECIFIC ENERGY OF SCRATCHING

3.3.1. *Theoretical analysis*

The specific energy of scratching is defined as the energy for removing a unit volume of material. In the single-point scratch test, the configuration of the groove can be defined easily (Figure 8), and hence the total energy in scratching is simply the product of the tangential force (F_t) and the scratch length (L). The total volume of material removed by the indenter is equal to the scratch length by the cross-sectional area of the groove (A_s), Figure 8. Therefore, the specific energy of scratching can be calculated by

$$\mu = \frac{F_t L}{A_s L} = \frac{F_t L}{h^2 \tan \theta L} = \frac{F_t}{h^2 \tan \theta},$$ (1)

where h is the depth of cut and θ the semi-included angle of the groove.

Now let us consider theoretically the relationship between the specific energy of scratching and the depth of cut and material properties. According to the scratching process mentioned in Section 3.2, the energy of scratching can be expressed as

$$\mu = \mu_r + \mu_p + \mu_c + \mu_f,$$ (2)

where $\mu_r, \mu_p, \mu_c,$ and μ_f are the specific energy for rubbing, ploughing, plastic cutting and particle fracture respectively. To calculate μ, we must first find all the components on the right hand side of Equation (2).

In a grinding process, the tangential force for rubbing, F_t, could be expressed as a function of the depth of cut [18], h,
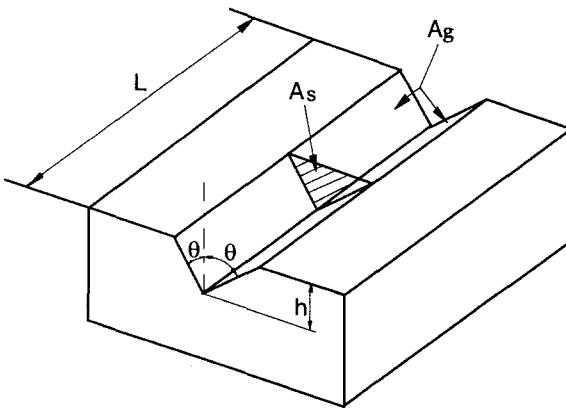
$$F_t = C_0 f p h^{1/2},$$ (3)

Fig. 8. Schematic diagram of a scratched groove.

where C_0 is a geometrical constant of grinding wheel, f is the friction coefficient and p the average contact stress. When the width of groove is larger than the tip radius of the indenter, f is constant and is determined only by the geometry of the indenter [19]. In this study, because of the apparent plastic deformation in the groove surface (Section 3.2), p could be assumed to be proportional to the yield stress of a composite [16]. Considering the similarity between a single-point scratching and a grinding process when only one cutting edge is involved, the specific energy of rubbing in scratching can be expressed as

$$\mu_r = \frac{F_t}{h^2 \tan \theta} = \frac{C_0 f p h^{1/2}}{h^2 \tan \theta} = \frac{C_1 \sigma_y}{h^{3/2}}, \tag{4}$$

where σ_y is the yield stress of the composite and C_1 a constant dependent on the geometry of the indenter only.

The mechanism of ploughing and plastic cutting processes is plastic deformation of the workmaterial [20, 21]. These processes take place simultaneously, thus the tangential force for ploughing and cutting for a composite material could reasonably be assumed to be proportional to the yield stress of the composite and the cross-sectional area of the groove. Therefore, the specific energy of ploughing and plastic cutting is

$$\mu_p + \mu_c = \frac{F_t}{h^2 \tan \theta} = \frac{C_2 \sigma_y A_s}{h^2 \tan \theta} = \frac{C_2 \sigma_y h^2 \tan \theta}{h^2 \tan \theta} = C_2 \sigma_y, \tag{5}$$

where C_2 is a constant.

The final component to be calculated is the specific energy of particle fracture. In the scratching process, the initial interaction between the indenter and a ceramic particles may be regarded as a point contact. According to the indentation fracture mechanics, radial and lateral cracks can be initiated beneath the indenter [22]. After the indenter passed, the cracks may propagate into the surface of the particle due to the residual stress field. Thus the particles in a composite was actually fractured by crack propagation, Figure 6a. Also, some particles were dug out by the moving indenter, Figure 6b. The relationship between the length of a radial crack and external load can be expressed as [22]

$$C = \alpha \frac{(E/H)^{2/5}}{K_c^{1/2} H^{1/8}} P^{5/8}, \tag{6}$$

where H is the Vicker's hardness of ceramics, E the Young's modulus, K_c the fracture toughness, P the indentation load and α a material-independent constant which depends on the shape of the indenter.

According to Griffith theory, the energy needed to propagate a crack should equal to the surface energy on the crack surface created. Because the dimension of a crack surface in a particle fractured or dug out by the indenter is of the same order of magnitude as the radial cracks, it is reasonable to assume that the
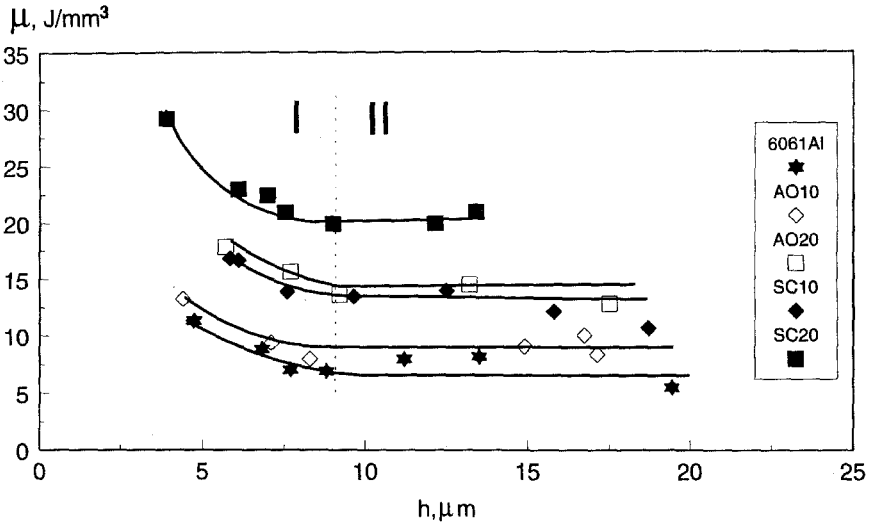
Fig. 9. Variation of specific energy with depth of cut.

specific energy of particle fracture is

$$\mu_f = \frac{KC\gamma L}{h^2 \tan \theta L} = \frac{KC\gamma}{h^2 \tan \theta},$$ (7)

where γ is the unit surface energy of the particles and K a constant related to the crack geometry and the number of cracks generated in a unit scratch length. Furthermore, the relationship between the indentation load and Vicker's hardness of a particle is

$$P = \alpha_1 H h^2,$$ (8)

α_1 is a geometrical constant. Combining Equations (6), (7) and (8), the expression of μ_f can be simplified to

$$\mu_f = \frac{C_3}{h^{3/4}},$$ (9)

where C_3 is a constant determined by material properties (E, H, K_c and γ), geometry of indenter (α, α_1 and θ) and crack geometry and number of cracks generated in unit scratch length (K).

Substituting Equations (4), (5) and (9) into (2), the total specific energy during scratching becomes

$$\mu = \frac{C_1 \sigma_y}{h^{3/2}} + C_2 \sigma_y + \frac{C_3}{h^{3/4}}.$$ (10)

3.3.2. *Size effect*

The variation of specific energy of scratching (after T6 treatment) with the depth of cut, h, is demonstrated in Figure 9. The specific energies for all the materials decrease with the increase of h in the regime of $h \leqslant 9 \, \mu m$ (regime I) and then keep almost constants (regime II). Therefore, there is an apparent size effect. Over the whole range of depth of cut, SC20 has the greatest specific energy of scratching and 6061 Al the least. This indicated that SC20 has the highest abrasive wear resistance among the materials studied.

In Equation (10), the contribution of rubbing, $C_1 \sigma_y / h^{3/2}$, to the total specific energy would become smaller with increasing h. This is consistent with the result of grinding on single phase materials [12]. The component due to ploughing and plastic cutting, $C_2 \sigma_y$, is independent of h. The contribution of particle fracture, $C_3 / h^{3/4}$, similar to the specific energy of rubbing, decreases with increasing h as well. Therefore, as shown in Figure 9, when h reaches a certain value, say $9 \, \mu m$, the effects of rubbing and particle fracture become negligible and the total specific energy of scratching remains a constant for a given composite material. This is in agreement with the formation of groove topography when the normal scratching load varies, as discussed in Section 3.2.

6061 Al is a single phase material and is also the matrix of the composites studied. A comparison of the behaviour of 6061 Al with the composites would therefore offer further understanding. Obviously, the specific energy of scratching 6061 Al does not have the particle fracture term in Equation (10). Moreover, for either 6061 Al or a composite, the specific energies of rubbing, ploughing and plastic cutting are proportional to the yield stress. Therefore, the summation of μ_r, μ_p and μ_c of scratching a composite can be obtained from that of scratching 6061 Al, provided that the yield stress of the latter is modified to that of the composite. According to the published data [23, 24], the yield stress of AO10, AO20, SC10 and SC20 is 298, 335, 305 and 360 MPa, respectively. Thus, μ_f of a composite can be distinguished by subtracting the modified scratching energy of 6061 Al from the total specific energy of the composites.

The variation of μ_f with h (regime I), is shown in Figure 10, which demonstrates that those of AO10 and AO20 are almost independent of $h^{-3/4}$, but those of SC10 and SC20 are linear increasing functions of $h^{-3/4}$. This indicates that at small h, particle fracture has only negligible effect on the size effect when scratching AO10 and AO20 but becomes more obvious when scratching SC20 and SC10.

3.3.3. *Effect of volume fraction and particle size*

The above difference of specific energy of scratching AO and SC composites is mainly due to the different volume fraction and particle size of the reinforcement. Assuming that particles are spherical and with radius R, the total edge length of
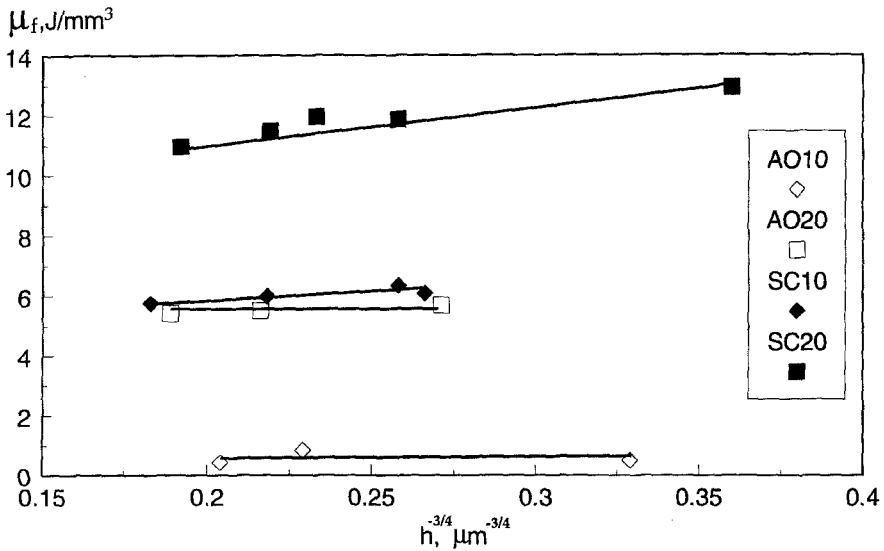
μ_f,J/mm^3

Fig. 10.   Variation of μ_f with depth of cut.

the particles on the groove surface (A_g, Figure 8) can be expressed as [25]:

$$L_e = \frac{3\pi f_\nu A_g}{4R} = \frac{3\pi}{4} A_g \xi, \tag{11}$$

where L_e is the total edge length of the particles, f_ν the volume fraction and ξ is the ratio of volume fraction to particle radius, as defined in Section 3.1. The total edge length of particles on the groove surface, or, the probability of ceramic particles encountered by the indenter is proportional to ξ. The values of ξ of SC20, SC10, AO20 and AO10 are respectively 14.2, 8.1, 2.9 and 2.2, Table I. Clearly, SC20 has the greatest ξ among all the materials. This is why for SC20, particle fracture has an obvious effect on the specific energy and the size effect at small h. However, the size effect in AO10 and AO20 is caused by rubbing rather than particle fracture. Because SC10 has an intermediate value of ξ, particle fracture still has a small contribution to the size effect. At large depths of cut (regime II), the effect of reinforcement on specific energy is mainly through their influence on the compound hardness.

Based on the relationship between depth of cut and specific energy as well as groove topography, for machining MMCs, a large depth of cut should be recommended to maintain a minimum specific machining energy, especially for those with larger ξ values.

4. Conclusions

(1) The single-point scratching process of 6061 Al reinforced by 10%, 20%, Al_2O_3/SiC ceramic particles is governed by a combined effect of rubbing, ploughing, plastic cutting and particle fracture. The apparent size effect can be interpreted clearly by the simple model of specific scratching energy.

(2) At a small depth of cut, the high specific energy and irregular groove topography are caused by both particle fracture and rubbing for the material with high ratio of volume fraction to particle radius (ξ), but mainly by rubbing for those with low values of ξ and those with single phase. 6061 Al reinforced by 20% SiC, which has the largest compound hardness and ξ value, has the greatest specific energy of scratching. At a large depth of cut, the specific energy of scratching and groove topography are mainly controlled by ploughing and plastic cutting and are independent of the depth of cut.

(3) For machining MMCs, a larger depth of cut should be recommended to maintain a minimum machining energy, especially for those with larger ξ values.

Acknowledgements

References

1. Hosking, M. F. *et al.*, 'Composites of Aluminium Alloys: Fabrication and Wear Behaviour', *J. Mat. Sci.* **17**, 1982, 477–498.
2. Sato, A. and Mehrabian, R., 'Aluminium Matrix Composites: Fabrication and Properties', *Metall Trans.* **7B**, 1976, 443–451.
3. Banerji, A., Surappa, M. K. and Rohatgi, P. K., Cast Aluminium Alloys Containing Dispersions of Zircon Particles', *Metall Trans.* **14B**, 1983, 273–283.
4. Lin, S. J. and Liu, K. S., 'Effect of Aging on Abrasive Rate in an Al–Zn–Mg–SiC Composite', *Wear* **121**, 1988, 1–14.
5. Wang, A. G. and Hutching, I. M., 'Wear of Alumina Fibre-Aluminium Matrix Composites by Two-Body Abrasion', *Mat. Sci. Tech.* **5**, 1989, 71–75.
6. Tonshoff, H. K., Peters, J., Inasaki, I. and Paul, T., 'Modelling and Simulation of Grinding Processes', *Annals of the CIRP* **41**(2), 1992, 677–688.
7. Malkin, S. and Anderson, R. B., 'Thermal Aspects of Grinding: Part I-Energy Partition', *J. of Engineering for Industry* **96**, 1974, 1177–1191.
8. Backer, W. R., Marshall, E. R. and Shaw, M. C., 'The Size Effect in Metal Cutting', *Trans. ASME* **74**, 1952, 61–72.
9. Brecker, J. N. and Shaw, M. C., 'Specific Energy in Single Point Grinding,' *Annals of the CIRP* **23**, 1974, 93–94.
10. Broese van Groenou, A., Maan, N. and Veldkamp, J. D. B., 'Scratching Experiments on Various Ceramic Materials', *Philips. Res. Rep* **30**, 1975, 320–359.
11. Nakayama, K. and Tamura, K., 'Size Effect in Metal Cutting Force', *J. of Engineering for Industry* **90**, 1968, 119.
12. Malkin, S. *et al.*, 'Size Effect in Abrasive processes', in F. Koenigsberger and S. A. Tobias (eds), *Proceeding of the 13th International Conference on Machine Tool Design and Research,* MacMillan, Birmingham, 1972, pp. 291–296.

13. Clyne, T. W. and Withers, P. J., *An Introduction to Metal Matrix Composites,* Cambridge University Press, Cambridge, 1993.
14. Glormini, P. and Felder, E., 'Theoretical and Experimental Study of the Ploughing of a Rigid-Plastic Semi-Infinite Body by a Rigid Pyramidal Indenter', *Wear* **88**, 1983, 195–206.
15. Kato, K. *et al.*, 'Three-Dimensional Shape Effect on Abrasive Wear', *J. of Tribology* **108**, 1988, 346.
16. Johnson, K. L., *Contact Mechanics,* Cambridge University Press, Cambridge, 1985.
17. Zhang, L. C. and Moffid, M., 'A Numerical Investigation into the Micro-Indentation of Silicon', in C. C. Sorrell and A. J. Ruys (eds), *International Ceramic Monographs,* Australasian Ceramic Society, Sydney, 1994, pp. 644–650.
18. Malkin, S., *Grinding Technology-Theory and Application of Machining with Abrasives*, Wiley, New York, 1989.
19. Sin, H., Saka, N. and Suh, N. P., 'Abrasive Wear Mechanisms and the Grit Size Effect', *Wear* **55**, 1979, 163–190.
20. Kosel, T. H., 'Review of Scratch Rest Studies of Abrasive Mechanisms', in P. J. Blau and B. R. Lawn (eds), *Microindentation Techniques in Materials Science and Engineering*, International Metallographic Society, Philadelphia, 1986, pp. 227–242.
21. Moore, M. A., 'Abrasive Wear', in D. A. Rigney (ed.), *Fundamentals of Friction and Wear of Materials,* American Society for Metal, Ohio, 1981, pp. 73–118.
22. Evans, A. G. and Marshall, D. B., 'Wear mechanism in Ceramics', in D. A. Rigney (ed.), *Fundamentals of Friction and Wear of Materials,* American Society for Metal, Ohio, 1981, pp. 439–454.
23. McDanels, D. L., 'Analysis of Stress-Strain, Fracture and Ductility of Aluminium Matrix Composites Containing Discontinuous Silicon Carbide Reinforcement', *Metall. Trans.* **16A**, 1985, 1105–1115.
24. Hadianfard, M. J., 'Mechanical Properties, Fracture and Fatigue Behaviour of Aluminium-Based Metal Matrix Composites', PhD Thesis, University of Sydney, 1994.
25. Kulik, T. and Kosel, T. H., 'Effects of Second-Phase particle Size and Edge Microfracture on Abrasion of Model Alloy', in K. C. Ludema (ed.), *Wear of Materials,* ASME, Colorado, 1989, pp. 71–78.